https://doi.org/10.5194/egusphere-2022-1487
Preprint. Discussion started: 2 January 2023

Water release and homogenization by dynamic recrystallization of quartz

Junichi Fukuda[1], Takamoto Okudaira[1], Yukiko Ohtomo[2]

[1]Department of Geosciences, Osaka Metropolitan University, Osaka, 558-8585, Japan
[2]Department of Education, Art and Science, Yamagata University, Yamagata, 990-8560, Japan

Correspondence to: Junichi Fukuda (jfukuda@omu.ac.jp)

Abstract. To evaluate changes in water distribution generated by dynamic recrystallization of quartz, we performed infrared (IR) spectroscopy mapping of quartz in deformed granite from the Wariyama uplift zone in NE Japan. We analyzed three granite samples with different degrees of deformation: almost undeformed, weakly deformed, and strongly deformed. Dynamically recrystallized quartz grains with a grain size of ~10 μm are found in these three samples, but the percentages of recrystallized grains and recrystallization processes are different. Quartz in the almost undeformed sample shows wavy grain boundaries with a few bulged quartz grains. In the weakly deformed sample, bulging of quartz is developed in regions a few hundred micrometers from adjacent host quartz grains. In the strongly deformed sample, almost all quartz grains are recrystallized by subgrain rotation. IR spectra of quartz in the three samples commonly show a broad water band owing to H_2O fluid at 2800–3750 cm^{-1} with no structural OH bands. Water contents in host quartz grains in the almost undeformed sample are in the range of 40–1750 wt. ppm, with a mean of 500 ± 280 wt. ppm H_2O. On the other hand, water contents in regions of recrystallized grains, regardless of the recrystallization processes involved, are in the range of 100–510 wt. ppm, with a mean of 220 ± 70 wt. ppm, which are low and homogeneous compared with contents in host quartz grains. Water contents in regions of subgrains are intermediate between those in host and recrystallized grains. These results for water distribution in quartz imply that water is released by dynamic recrystallization.

1 Introduction

Quartz is a major constituent of Earth's crust, and its deformation can control crustal rheology (e.g., Rutter and Brodie, 1988; Kohlstedt et al., 1995; Bürgmann and Dresen, 2008; Fossen and Cavalcante,

https://doi.org/10.5194/egusphere-2022-1487
Preprint. Discussion started: 2 January 2023

2017). For plastic deformation of quartz, water occurring as an impurity in this mineral can reduce its strength by up to a few orders of magnitude, as has been confirmed by numerous experimental investigations (e.g., Griggs and Blacic, 1965; Griggs, 1967; Blacic, 1975; Parrish et al., 1976; Jaoul et al., 1984; Kronenberg and Tullis, 1984; Koch et al., 1989; Post et al., 1996; Chernak et al., 2009; Holyoke and Kronenberg, 2013). In addition, increasing water fugacity reduces the plastic strength of quartz (Post et al., 1996; Chernak et al., 2009; Holyoke and Kronenberg, 2013; Fukuda and Shimizu, 2017; Fukuda et al., 2018; Tokle et al., 2019; Lu and Jiang, 2019; Lusk et al., 2021). As a species of water, molecular H_2O is trapped as fluid inclusions and at grain boundaries, and the crystal structure of quartz incorporates OH groups that are coupled with impurity cations in quartz (Kats, 1962; Aines and Rossman, 1984; Kronenberg, 1994; Stenina, 2004; Stalder, 2021; also see the review by Stünitz et al., 2017, for water species in quartz and their effects on plastic deformation).

Water in naturally deformed quartz has been measured by infrared (IR) spectroscopy focusing on contents and species (H_2O or OH) (Kronenberg and Wolf, 1990; Kronenberg et al., 1990; Kronenberg, 1994; Nakashima et al., 1995; Niimi et al., 1999; Muto et al., 2004, 2005; O'Kane et al., 2007; Gleason and DeSisto, 2008; Menegon et al., 2011; Finch et al., 2016; Kilian et al., 2016; Kronenberg et al., 2017, 2020; Fukuda and Shimizu, 2019). However, the effects of water content and species in quartz on the strength of quartz are not fully understood, especially regarding the quantitative relationships between water content, species, and flow laws of quartz. These relationships in olivine have been partly evaluated by experimental means (Jung and Karato, 2001; Hirth and Kohlstedt, 2003; Katayama et al., 2004; Jung et al., 2006; Masuti et al., 2019) and have been linked to the deformation of natural olivine and to mantle dynamics (Karato et al., 2008; Katayama et al., 2011; Skemer et al., 2013; Jung, 2017).

IR spectroscopic measurements of water in quartz have revealed that water content increases with decreasing grain size (Kronenberg and Wolf, 1990; Kronenberg et al., 1990; Kronenberg, 1994; Nakashima et al., 1995; Muto et al., 2004, 2005; Fukuda and Shimizu, 2019), which has been explained in terms of volume increases of grain boundaries being able to host more water than intracrystalline parts (Ito and Nakashima, 2002). It is also known that grain size can be reduced by dynamic recrystallization (reviewed for quartz in, e.g., Stipp et al., 2002; Tullis, 2002; Passchier and Trouw, 2005). Recent studies of naturally deformed quartz by Finch et al. (2016) and Kronenberg et al. (2020) have shown that water content decreases as grain size decreases by dynamic recrystallization, on which basis those authors proposed that water is released by dynamic

https://doi.org/10.5194/egusphere-2022-1487
Preprint. Discussion started: 2 January 2023

recrystallization. The release of water by dynamic recrystallization has also been shown by the experiments of Palazzin et al. (2018). Those various studies performed point IR analyses in regions composed of dynamically recrystallized quartz grains. However, there is still only limited information on water contents, species, and distributions with the development of texture, meaning that more data are required for water distributions in naturally deformed quartz.

In this study, we performed IR mapping analyses of undeformed quartz grains and dynamically recrystallized grains. We use the results as a basis for discussion of variations in water content and the behavior of water release arising from textural change due to dynamic recrystallization.

2 Samples

Granite samples with differing degrees of deformation were obtained from the Wariyama uplift zone in NE Japan, which is located on the eastern side of the Futaba Fault (Fig. 1). The geological setting of this zone has been reported by Oide and Fujita (1975) and Fujita et al. (1988). Tsuchiya et al. (2014) reported a U–Pb zircon age of ca. 300 Ma for the Wariyama granite and documented an age of ca. 120 Ma for the Takase granite to the eastern side of the Wariyama granite. The deformed Wariyama granite is found on the eastern side of the Takase Pass as a local shear zone (Tsuchiya et al., 2013). We divided the deformed Wariyama granite samples into three types—almost undeformed, weakly deformed, and strongly deformed—on the basis of the development of foliations of mylonitic rocks by the naked eye (Fig. 2) and of microstructures under a polarizing microscope (Fig. 3).

The almost undeformed sample preserves the original igneous texture (Figs 2 and 3a), and original quartz grains of up to 2 mm in size are observed. However, quartz grain boundaries are wavy, and a few bulged grains of ~10 μm occur (Fig. 3b). Therefore, we term this sample “almost” undeformed. In original quartz grains, fluid inclusions are observed and are heterogeneously distributed (Fig. 3b). In the weakly deformed sample cut parallel to the lineation and perpendicular to the foliation, larger regions of a few hundred micrometers are composed of bulged quartz grains that have developed from adjacent elongated host quartz grains (Fig. 3c and d). In comparison with the almost undeformed sample, there are fewer large fluid inclusions. Thus, the redistribution of fluid inclusions by deformation is inferred, as reported previously in natural samples (Kerrich, 1976; Wilkins and Barkas, 1978; Hollister, 1990; Cordier et al., 1994; Vityk et al., 2000; Faleiros et al., 2010). According to those previous studies, fluid inclusions may undergo leakage or smaller

https://doi.org/10.5194/egusphere-2022-1487
Preprint. Discussion started: 2 January 2023

inclusions or structural OH may be formed, as confirmed experimentally by Stünitz et al. (2017) and Palazzin et al. (2018). In this study, we examine the actual water distribution by using IR spectroscopic measurements. The strongly deformed sample shows well developed foliations (Fig. 2) and almost fully recrystallized quartz texture (Fig. 3e and f). Recrystallized quartz grains measuring ~10 μm in size and formed by subgrain rotation constitute the major part of the quartz matrix (Fig. 3e). In some regions of quartz, crystallographic orientations continuously change as in undulose extinction, and these regions are composed of subgrains (Fig. 3f).

Grain sizes of recrystallized grains were determined by imaging. More than 300 grains of recrystallized grains in optical photomicrographs (e.g., Fig. 3b, d, and f) were traced. The area of each grain was determined by image analysis using ImageJ software, and grain size was expressed as an equivalent circle diameter. The mean grain sizes of recrystallized quartz with ±1 standard deviation of the almost undeformed, weakly deformed, and strongly deformed samples are 10.5 ± 3.7, 6.7 ± 1.9, and 9.6 ± 3.6 μm, respectively (Fig. 4). The piezometers of Stipp and Tullis (2003) and Holyoke and Kronenberg (2010) developed for bulging recrystallization were applied to the mean grain sizes of the almost undeformed and weakly deformed samples and they yield values of a few tens of megapascals. Similarly, values of a few hundred megapascals are obtained for the mean grains size of the strongly deformed sample using the piezometers of these two papers and others (Twiss, 1977; Shimizu, 2008, 2012; Cross et al., 2017) for subgrain rotation.

3 Analytical procedure for IR spectroscopy

Quartz grains in the almost undeformed, weakly deformed, and strongly deformed samples were measured by IR mapping to evaluate water contents and species. Sample thin sections with an approximate thickness of 100 μm were prepared by dissolving glycol phthalate resin in acetone. Subsequently, the actual sample thicknesses of the IR mapped areas were measured using a dial gauge attached to a stand. The sample thickness of approximately 100 μm is suitable for obtaining good transmitted IR signals through quartz and for making textural observations under a polarizing microscope.

We used a Fourier-transform IR spectrometer (JASCO FT/IR-4700) equipped with a microspectrometer (JASCO IRT-5200) to measure water included in quartz and other minerals in the samples. The IR spectrometer incorporated a silicon carbide (Globar) IR source and KBr beamsplitter. Unpolarized IR light was irradiated to the sample set on the sample stage of the

https://doi.org/10.5194/egusphere-2022-1487
Preprint. Discussion started: 2 January 2023

microspectrometer, and IR light through the sample under atmospheric conditions was detected using a mercury–cadmium–telluride detector in the microspectrometer. IR spectra were obtained from an average of 100 scans with a wavenumber resolution of 4 cm^{-1}. An aperture size of 25 × 25 μm was used. Mapping measurements were performed using a beam-moving function in the sample area of up to 400 × 400 μm. Mapping step intervals the same as the aperture size were applied. We checked that mapping measurements with larger aperture sizes for the same areas gave similar averaged water distributions. We also included other minerals such as plagioclase and/or phyllosilicate neighboring quartz in the mapping, as their IR spectra differ substantially from those of quartz and can serve as markers in IR mapped data to match with the locations in the optical photomicrographs.

Water contents were converted from absorbance of water stretching bands with linear baselines from 2800 to 3750 cm^{-1}. Water stretching bands in our quartz samples commonly exhibit molecular H_2O bands (presented below in the Result section). We used the calibration of Paterson (1982) designed for molecular H_2O as $C = \int A(\nu)/100(3780 - \nu)d\nu$, where C is the concentration in mol H_2O ℓ^{-1} (Note that the original paper of Paterson (1982) uses H ℓ^{-1}), and $A(\nu)$ is the absorbance at a wavenumber ν in cm^{-1} for a sample thickness normalized to 1 cm. Other calibrations for contents of molecular H_2O and/or OH species in quartz have been given by Kats (1962), Aines et al. (1984), Nakashima et al. (1995), Libowitzky and Rossman (1997), Stipp et al. (2006), and Thomas et al. (2009). Fukuda and Shimizu (2019) compared these calibrations, and the ratio of calculated water contents between them based on Paterson (1982) as unity are 0.68:0.88:1.15:1.31:1.58:0.43. In this study, water contents are expressed as wt. ppm H_2O.

4 Results

The results of IR mapping for the almost undeformed sample are shown in Fig. 5. The measured area includes a single quartz grain (Fig. 5a). Water contents are heterogeneous (Fig. 5b), ranging from a minimum of 40 wt. ppm (No. 1) to a maximum of 1750 wt. ppm (No. 5), the raw IR spectra for which are presented in Fig. 5c. The heterogeneous distribution of fluid inclusions is clearly observed in the optical photomicrograph (Fig. 3b) and would correspond to the IR mapped data. Raw IR spectra commonly show a broad band at 2800–3750 cm^{-1}, which is a result of the stretching vibrations of molecular H_2O (Fig. 5c).

https://doi.org/10.5194/egusphere-2022-1487
Preprint. Discussion started: 2 January 2023

The results of IR mapping for the weakly deformed sample are presented in Fig. 6. The measured area includes two host quartz grains, dynamically recrystallized grains around them, and plagioclase grains (Fig. 6a). In the water distribution map (Fig. 6b), plagioclase shows much higher water contents (around No. 5) compared with quartz. The higher water contents in plagioclase in the mapped data serve as a marker for comparison with the textural image (Fig. 6a). The IR spectrum of plagioclase in Fig. 6c shows a sharp band at 3630 cm^{-1}, which may be related to structural hydroxyl vibration(s) of plagioclase and/or altered clay minerals (Johnson and Rossman, 2004). Water contents in the host grains are in the range of 600–1000 wt. ppm (Fig. 6b). In contrast, water contents in the recrystallized regions are 200–300 wt. ppm, clearly lower than those in the host grains. In addition, a gradual decrease in water content from the host grains to the adjacent recrystallized regions is observed in some cases; for example, over a distance of ~150 μm from No. 3 (host; 680 wt. ppm in Fig. 6c) to No. 1 (recrystallized region; 210 wt. ppm). In terms of texture, this decrease is consistent with the development of dynamic recrystallization from subgrains in and around host grains (Fig. 6a) to recrystallized grains.

In another part of the weakly deformed sample (Fig. 7), subgrains are seen at certain sample stage angles under a polarizing microscope (Fig. 7a and b). Water contents in recrystallized regions including subgrains are 290–500 wt. ppm (around Nos 1 and 2 in Fig. 7c and d), slightly higher than those in the recrystallized regions in Fig. 6. Water contents in host grains range up to 1540 wt. ppm, which is as high as those in the almost undeformed sample.

The results of IR mapping for the strongly deformed sample are shown in Fig. 8. The IR mapped area consists mainly of recrystallized quartz and partly of subgrains whose crystallographic orientations look continuously similar and/or continuously change as in undulose extinction (Fig. 8a). Water contents in the subgrain region (around No. 4 in Fig. 8b) are 390–540 wt. ppm, substantially higher than those in other recrystallized regions (water contents of 120–250 wt. ppm). The IR spectra of quartz in the strongly deformed sample commonly show a broad H_2O band at 2800–3750 cm^{-1} (Fig. 8c), the same as quartz in the almost undeformed and weakly deformed samples (Figs 5–7). The low and homogeneous water contents in the recrystallized regions are consistent with those in the weakly deformed sample (Fig. 6).

https://doi.org/10.5194/egusphere-2022-1487
Preprint. Discussion started: 2 January 2023

5 Discussion

5.1 Water in host quartz and water species

Water contents in host quartz grains are heterogeneous regardless of the degree of deformation (Figs 5–7) and range from 40 to 1750 wt. ppm with a mean of 500 ± 280 wt. ppm in the almost undeformed sample and from 250 to 1540 wt. ppm with a mean of 800 ± 200 wt. ppm in the weakly deformed sample (Fig. 9). The IR spectra commonly show a broad band at 2800–3750 cm^{-1} as molecular H_2O, which is presumed to correspond to fluid inclusions in quartz grains observed in the optical photomicrograph (Fig. 3b). In contrast, fluid inclusions in host quartz grains in the weakly deformed sample are less numerous in the photomicrograph (Fig. 3d). As water contents in host quartz grains in the almost undeformed and weakly deformed samples do not differ, a redistribution of fluid inclusions with a size change to less than the optical microscopic scale must have occurred in the latter sample. The redistribution of fluid inclusions owing to plastic deformation has been reported in previous textural observations (Kerrich, 1976; Wilkins and Barkas, 1978; Hollister, 1990; Cordier et al., 1994; Vityk et al., 2000; Faleiros et al., 2010). Some of those studies proposed leakage of water during the redistribution of fluid inclusions, but this is unlikely to have been significant in the host grains analyzed in the present study since the water contents in host grains in the almost undeformed and weakly deformed samples are not significantly different. In the IR mapping images for the weakly deformed sample, the high-water-content regions (Figs 6a and 7a and b) are comparable to relics of host grains identified under a polarizing microscope (Figs 6b and 7c). In comparison, in the almost undeformed sample, water contents in host grains are simply heterogeneous. Therefore, in the weakly deformed sample, the higher mean water contents in host grains may also be due to the redistribution of fluid inclusions. The redistribution of fluid inclusions has similarly also been reported from IR spectroscopic measurements of an experimentally deformed single quartz crystal (Stünitz et al., 2017). Those authors demonstrated that original fluid inclusions with sizes of up to 100 μm transformed into OH dislocations that showed a sharp band at 3585 cm^{-1} in IR spectra. This band was also observed in naturally deformed quartz by Niimi et al. (1999) and Gleason and DeSisto (2008) but was not detected in our samples or others (e.g., Kronenberg and Wolf, 1990; Kronenberg et al., 1990; Muto et al., 2004, 2005; O'Kane et al., 2007; Finch et al., 2016; Kronenberg et al., 2017, 2020; Fukuda and Shimizu, 2019). Stünitz et al. (2017) also demonstrated that these OH dislocations, which could have originally been visible fluid inclusions

https://doi.org/10.5194/egusphere-2022-1487
Preprint. Discussion started: 2 January 2023

with sizes of a few micrometers under an optical microscope, are again transformed into much smaller fluid inclusions measuring less than 100 nm in size by subsequent annealing. This process may have occurred in our samples and can explain the redistribution of fluid inclusions in the optical photomicrographs (Fig. 3b vs. 3d) while retaining the original water contents.

5.2 Water in dynamically recrystallized quartz

As seen in the weakly and strongly deformed samples, where dynamic recrystallization of quartz is developed, water contents in recrystallized regions are low and homogeneous compared with those in host grains (Figs 6–8). The mean water content is 220 ± 70 wt. ppm (Fig. 9) where grains are fully recrystallized. As the sizes of the recrystallized grains are ~10 μm (Fig. 4), and the sample thickness is ~100 μm, the aperture size of 25 × 25 μm of the IR microspectrometer captures both intracrystalline and grain boundary water. In the regions of subgrains in the weakly deformed sample (Figs 6 and 7) and in the strongly deformed sample (Fig. 8), water contents in subgrain regions are intermediate between those in recrystallized regions and host grains. Thus, water in quartz is inferred to be released by the development of dynamic recrystallization. Similar results have been reported by Finch et al. (2016) and Kronenberg et al. (2020) for naturally recrystallized quartz and by Palazzin et al. (2018) for experimentally recrystallized quartz. Kronenberg et al. (2020) reported that water contents in quartzites from the Moine thrust vary from around 600 to 220 wt. ppm depending on the percentage of recrystallized regions from 20% to 100% toward the thrust within a distance of 70 m. The mean recrystallized grain size in their samples was 21.7 μm. As those authors performed point analyses, it may be difficult to correlate the water content values with the microstructures, and their water content values may thus include subgrains, which are more likely to be measured when recrystallization percentages are low. In addition, in our weakly deformed sample, water contents in quartz gradually decrease with increasing distance from the adjacent host grains within a range of ~150 μm (Fig. 6), which may be due to the transition from subgrains to recrystallized grains. In addition, in the strongly deformed sample, water contents in regions of subgrains are higher than those in recrystallized regions (Fig. 8). Water contents reported by Finch et al. (2016) for deformed granitic diatexite vary from approximately 650 to 200 wt. ppm from their weakly deformed sample to mylonite to ultramylonite and with decreasing grain size from 95 to 60 μm (there are also slight differences in water contents between ribbon and matrix regions in their samples). Palazzin et al. (2018) reported water contents in matrix regions with a grain size of <10 μm in experimentally

https://doi.org/10.5194/egusphere-2022-1487
Preprint. Discussion started: 2 January 2023

deformed quartzite of ~200 wt. ppm, even though different starting quartz samples with different water contents ranging from 39 to 3446 wt. ppm were used (their table 1). In addition, Fukuda et al. (2012) found heterogeneously distributed water with contents of 150–2200 wt. ppm in K-feldspar porphyroclasts in granitoid mylonite. In contrast, in the same granitoid mylonite sample, water in regions of fine-grained K-felspar (~20 μm), which could have been formed by solution–precipitation processes around porphyroclasts, was homogeneously distributed with contents of 150–300 wt. ppm, much lower than those in porphyroclasts. Those authors also proposed that water was released during the formation process of fine grains.

If the water content of 220 ± 70 wt. ppm in the recrystallized regions analyzed in this study is distributed homogeneously in grain boundaries as thin films, then the mean grain size of ~10 μm (Fig. 4) gives a grain boundary width of ~2 nm based on the estimation by Ito and Nakashima (2002) (1.9 nm using their cubic grain model and 2.5 nm using their tetradecahedral grain model). This is consistent with the estimation by Palazzin et al. (2018) for their samples whose grain sizes are similar to ours. However, there is no basis for assuming homogeneous grain boundary films. Some previous studies of natural quartz aggregates have shown that water contents increase with decreasing grain size (Kronenberg et al., 1990; Nakashima et al., 1995; Ito and Nakashima, 2002; Muto et al., 2004, 2005; Fukuda and Shimizu, 2019). In these cases, where quartz displays textural modifications by dynamic recrystallization and/or grain growth, water may have been continuously supplied to fill grain boundaries, where more water can be stored compared with intracrystalline parts. Under natural conditions, including those of the upper and middle crust, fluid water could form thin films in quartz grain boundaries with a wetting angle of <60°, as confirmed by experiments (Watson and Brenan, 1987; Holness, 1992, 1993) and observations of natural samples (Hiraga et al., 1999). For example, in the IR mapping measurements reported by Fukuda and Shimizu (2019) for quartz in Sanbagawa metamorphic schist, the estimated water content varies from 310 to 40 wt. ppm in quartz aggregated regions with changing grain size from ~40 μm (chlorite zone) to ~120 μm (oligoclase–biotite zone). The water content in the latter sample is inferred to be from intracrystalline parts, as the grain size and sample thickness were sufficiently large for the aperture sizes of 30 × 30 μm or 50 × 50 μm used in those authors' study. For their samples whose grain sizes were smaller than the aperture sizes, the measured water would include grain boundaries. Their estimated grain boundary width filled with water was ~10 nm, which is approximately five times larger than that estimated in the present study. However, grain boundaries are not always filled with water, depending on the

https://doi.org/10.5194/egusphere-2022-1487
Preprint. Discussion started: 2 January 2023

water-available conditions after dynamic recrystallization. In our samples, quartz grain boundaries may not have undergone a subsequent water infiltration process, and the water distribution indicates that water contents in recrystallized regions include the water released from host grains by dynamic recrystallization.

5.3 Mechanism of water release and homogenization by dynamic recrystallization

In our samples, it is clear that water occurring as fluid inclusions in host quartz grains is released and homogenized by dynamic recrystallization (Figs 5–9). Fluid inclusions in host quartz grains may be trapped during quartz crystallization from magma. As experimentally confirmed by Tarantola et al. (2010), when plastic strain is very low (<1%), the shapes of fluid inclusions may be elongated or burst in the original locations. In contrast, under higher plastic strain when dislocations, which would be associated with the formation of hydroxyl, are introduced as Si–O–Si + H_2O ← → Si–OH ⋯ OH–Si, original fluid inclusions can be redistributed by diffusion, which is also rate-limited by this reaction (Kerrich, 1976; Wilkins and Barkas, 1978; Hollister, 1990; Cordier et al., 1994; Vityk et al., 2000; Faleiros et al., 2010). In addition to this type of diffusion, diffusion through dislocation cores (i.e., pipe diffusion) can redistribute fluid inclusions (Trepied and Doukhan, 1978; Cordier et al., 1988, 1994; Kronenberg, 1994). In cases where Si–OH is preserved, the IR spectrum shows its OH vibration at 3585 cm^{-1} (Stünitz et al., 2017) or at 3596 cm^{-1} (Niimi et al., 1999; Gleason and DeSisto, 2008). However, as discussed above, Si–OH transforms back to SiO_2 + H_2O by annealing to form smaller fluid inclusions with sizes of <100 nm both in host and recrystallized grains (Stünitz et al., 2017). Thus, the redistribution of fluid inclusions caused by diffusion may account for water distributions comparable to the shapes of host grains in the weakly deformed sample (Figs 6 and 7), as discussed in section 5.1. In cases where diffused H_2O during the redistribution process reaches newly formed grain boundaries by dynamic recrystallization, this water should be released, as grain boundaries are fast diffusion paths that lead to the development of equilibrium texture. During the dynamic recrystallization process from subgrains to fully recrystallized grains, the water release process may be enhanced by the development of fast diffusion paths. In fact, water contents in regions of subgrains are intermediate between those in host grains and regions of recrystallized grains (Figs 6–8), indicating that the degree of water release depends on the degree of dynamic recrystallization. Some studies have also speculated that water transfer including release can occur through microcracking (e.g., Kronenberg et al., 1986; Palazzin et al.,

https://doi.org/10.5194/egusphere-2022-1487
Preprint. Discussion started: 2 January 2023

2018), but this process was not confirmed in our samples. In summary, through dynamic recrystallization, water release and homogenization occur to achieve the equilibrium state corresponding to the deformation conditions.

6 Conclusions

We performed IR mapping measurements on host and recrystallized quartz in three types of Wariyama granite: almost undeformed, weakly deformed, and strongly deformed. Our results allow the following conclusions to be drawn:

• Water in host quartz grains in the almost undeformed sample has contents of 40–1750 wt. ppm, with a mean of 500 ± 280 wt. ppm, and is heterogeneously distributed as fluid inclusions.

• Fluid inclusions in host quartz grains in the weakly deformed sample become less numerous under a polarizing microscope compared with those in almost undeformed sample. The water contents of host quartz grains in the two samples do not change substantially, but the water distributions in host grains in the weakly deformed sample can be comparable to the shapes of host grains. This suggests a redistribution of water within host grains during plastic deformation.

• When dynamic recrystallization occurs, water is mostly likely released along newly formed grain boundaries by diffusion and homogenized to achieve an equilibrium state. Water contents in regions of recrystallized grains are 100–510 wt. ppm, with a mean of 220 ± 70 wt. ppm.

• Water contents in regions of subgrains are intermediate between those in host grains and recrystallized regions, implying that the degree of water release depends on the degree of dynamic recrystallization.

Data availability. Raw IR mapped data for Figs 5–8 in JASCO format (e.g., Fig5.jwa) and each exported IR spectrum for each sample position (e.g., Fig5_X1Y1.txt) are available from Mendeley Data at https://data.mendeley.com/datasets/zn24kbg9xt/draft?a=3552fbc3-364c-4edd-b50a-fa58d198bcce [Comment from authors: This is a temporary shared URL. We will officially publish

https://doi.org/10.5194/egusphere-2022-1487
Preprint. Discussion started: 2 January 2023

the data in Mendeley Data when the manuscript is published as an article in Solid Earth]. These data can be used to reproduce the water content variations presented in Fig. 9.

Sample availability. The samples used in this study are available at the locations shown in Fig. 1. The rock specimens for Fig. 2 and thin sections for Fig. 3 and Figs 5–8 (IR analyses) are stored in the laboratory of JF. The thin sections for Fig. 3 were used for the grain size analyses presented in Fig. 4.

Author contributions. JF conceptualized the study, performed the formal analyses for all data, and carries overall responsibility for the study. JF and YO investigated the geological setting. All authors investigated the sample microstructures. JF and TO analyzed the IR data. JF drafted the main part of the paper. All authors drafted, reviewed, and edited the paper.

Competing interests. The authors declare that they have no conflicts of interest.

Acknowledgments. This research was supported by a Grant-in-Aid for Scientific Research (KAKENHI 19K04041 for JF and 20K04087 for TO) provided by the Japan Society for the Promotion of Science (JSPS).

References

Aines, R. D., Kirby, S. H., and Rossman, G. R.: Hydrogen speciation in synthetic quartz, Phys. Chem. Miner., 11, 204–212, https://doi.org/10.1007/BF00308135, 1984.

Aines, R. D. and Rossman, G. R.: Water in minerals? A peak in the infrared, J. Geophys. Res. Solid Earth, 89(B6), 4059–4071, https://doi.org/10.1029/JB089iB06p04059, 1984.

Blacic, J. D.: Plastic deformation mechanisms in quartz: the effect of water, Tectonophysics, 27, 271–294, https://doi.org/10.1016/0040-1951(75)90021-9, 1975.

Bürgmann, R. and Dresen, G.: Rheology of the lower crust and upper mantle: evidence from rock mechanics, geodesy, and field observations. Annu. Rev. Earth Planet Sci., 36, 531–567, https://doi.org/10.1146/annurev.earth.36.031207.124326, 2008.

https://doi.org/10.5194/egusphere-2022-1487
Preprint. Discussion started: 2 January 2023

Chernak, L. J., Hirth, G., Selverstone, J., and Tullis, J.: Effect of aqueous and carbonic fluids on dislocation creep strength of quartz, J. Geophys. Res. Solid Earth, 114, B04201, https://doi.org/10.1029/2008JB005884, 2009.

Cordier, P., Boulogne, B., and Doukhan, J. C.: Water precipitation and diffusion in wet quartz and wet berlinite $AlPO_4$, Bull. Minéral., 111, 113–137, 1988.

Cordier, P., Doukhan, J. C., and Ramboz, C.: Influence of dislocations on water leakage from fluid inclusions in quartz: a quantitative reappraisal, Eur. J. Mineral., 6, 745–752, 1994.

Cross, A. J., Prior, D. J., Stipp, M., and Kidder, S.: The recrystallized grainsize piezometer for quartz: An EBSD-based calibration, Geophys. Res. Lett., 44, 6667–6674, https://doi.org/10.1002/2017GL073836, 2017.

Faleiros, F. M., Campanha, G. A. da C., Ballo, R. M. da S., Fuzikawa, K.: Quartz recrystallization regimes, *c*-axis texture transitions and fluid inclusion reequilibration in a prograde greenschist to amphibolite facies mylonite zone (Ribeira Shear Zone, SE Brazil), Tectonophysics, 485, 193–214, https://doi.org/10.1016/j.tecto.2009.12.014, 2010.

Finch, M. A., Weinberg, R. F., and Hunter, N. J. R.: Water loss and the origin of thick ultramylonites, Geology, 44, 599–602, https://doi.org/10.1130/G37972.1, 2016

Fossen, H. and Cavalcante, G. C. G.: Shear zone –A review, Earth-Sci. Rev., 171, 434–455, http://dx.doi.org/10.1016/j.earscirev.2017.05.002, 2017.

Fujita, Y., Kano, H., Takizawa, F., and Yashima, R.: Geology of the Kakuda district. With geological sheet map at 1:50,000, Geol. Surv. Japan, 99 p. (in Japanese with English Abstract), 1988.

Fukuda, J., Holyoke, C. W., and Kronenberg, A. K.: Deformation of fine-grained quartz aggregates by mixed diffusion and dislocation creep, J. Geophys. Res., 123, 4676–4696, https://doi.org/10.1029/2017JB015133, 2018.

Fukuda, J., Okudaira, T., Satsukawa, T., and Michibayashi, K.: Solution-precipitation of K-feldspar in deformed granitoids and its relationship to the distribution of water, Tectonophysics, 532−535, 175−185, https://doi.org/10.1016/j.tecto.2012.01.033, 2012.

Fukuda, J. and Shimizu, I.: Theoretical derivation of flow laws for quartz dislocation creep: Comparisons with experimental creep data and extrapolation to natural conditions using water fugacity corrections, J. Geophys. Res., 122, 5956–5971, https://doi.org/10.1002/2016JB013798, 2017.

https://doi.org/10.5194/egusphere-2022-1487
Preprint. Discussion started: 2 January 2023

Fukuda, J. and Shimizu, I.: Water distribution in quartz schists of the Sanbagawa Metamorphic Belt, Japan: infrared spectroscopic mapping and comparison of the calibrations proposed determining water contents, Earth Planets Space, 71:136, https://doi.org/10.1186/s40623-019-1117-4, 2019.

Gleason, G. C. and DeSisto, S.: A natural example of crystal-plastic deformation enhancing the incorporation of water into quartz, Tectonophysics, 446, 16–30, https://doi.org/10.1016/j.tecto.2007.09.006, 2008.

Griggs, D. T.: Hydrolytic weakening of quartz and other silicates, Geophys. J. Int., 14, 19–31, https://doi.org/10.1111/j.1365-246X.1967.tb06218.x, 1967.

Griggs, D. T. and Blacic, J. D.: Quartz: Anomalous weakness of synthetic crystals, Science, 147, 292–295, https://doi.org/10.1126/science.147.3655.292, 1965.

Hiraga, T., Nagase, T., and Akizuki, M.: The structure of grain boundaries in granite-origin ultramylonite studied by high-resolution electron microscopy, Phys. Chem. Miner., 26, 617–623, https://doi.org/10.1007/s002690050226, 1999.

Hirth, G. and Kohlstedt, D.: Rheology of the upper mantle and the mantle wedge: A view from the experimentalists, in: Inside the Subduction Factory, edited by: Eiler, J., Geophys. Monogr. Ser., American Geophysical Union, 138, 83–105, https://doi.org/10.1029/138GM06, 2003.

Hollister, L. S.: Enrichment of CO_2 in fluid inclusions in quartz by removal of H_2O during crystal-plastic deformation, J. Struct. Geol., 12, 859–901, https://doi.org/10.1016/0191-8141(90)90062-4, 1990.

Holness, M. B.: Equilibrium dihedral angles in the system quartz–CO_2–H_2O–NaCl at 800°C and 1–15 kbar: the effects of pressure and fluid composition on the permeability of quartzites, Earth Planet. Sci. Lett., 114, 171–184, https://doi.org/10.1016/0012-821X(92)90159-S, 1992.

Holness, M. B.: Temperature and pressure dependence of quartz–aqueous fluid dihedral angles: the control of adsorbed H_2O on the permeability of quartzites, Earth Planet. Sci. Lett., 117, 363–377, https://doi.org/10.1016/0012-821X(93)90090-V, 1993.

Holyoke, C. W. and Kronenberg, A. K.: Accurate differential stress measurement using the molten salt cell and solid salt assemblies in the Griggs apparatus with applications to strength, piezometers and rheology, Tectonophysics, 494, 17–31, https://doi.org/10.1016/j.tecto.2010.08.001, 2010.

Holyoke, C. W. and Kronenberg, A. K.: Reversible water weakening of quartz, Earth Planet. Sci. Lett., 374, 385–390, http://dx.doi.org/10.1016/j.epsl.2013.05.039, 2013.

https://doi.org/10.5194/egusphere-2022-1487
Preprint. Discussion started: 2 January 2023

Ito, Y. and Nakashima, S.: Water distribution in low-grade siliceous metamorphic rocks by micro-FTIR and its relation to grain size: a case from the Kanto Mountain region, Japan, Chem. Geol. 189, 1–18, https://doi.org/10.1016/S0009-2541(02)00022-0, 2002.

Jaoul, O., Tullis, J., and Kronenberg, A.: The effect of varying water contents on the creep behavior of Hevitree quartzite, J. Geophys. Res. Solid Earth, B89, 4298–4312, https://doi.org/10.1029/JB089iB06p04298, 1984.

Johnson, E. and Rossman, G.R.: A survey of hydrous species and concentrations in igneous feldspars, Am. Mineral., 89, 586–600, https://doi.org/10.2138/am-2004-0413, 2004.

Jung, H.: Crystal preferred orientations of olivine, orthopyroxene, serpentine, chlorite, and amphibole, and implications for seismic anisotropy in subduction zones: a review, Geosci. J., 21, 985–1011, http://dx.doi.org/10.1007/s12303-017-0045-1, 2017.

Jung, H. and Karato, S.: Water-induced fabric transitions in olivine, Science, 293, 1460–1463, doi:10.1126/science.1062235, 2001.

Jung, H., Katayama, I., Jiang, Z., Hiraga, T., and Karato, S.: Effect of water and stress on the lattice-preferred orientation of olivine, Tectonophysics, 421, 1–22, doi:10.1016/j.tecto.2006.02.011, 2006.

Katayama, I., Jung, H., and Karato, S.: New type of olivine fabric from deformation experiments at modest water content and low stress, Geology, 32(12), 1045–1048, https://doi.org/10.1130/G20805.1, 2004.

Katayama, I., Michibayashi, K., Terao, R., Ando, J., and Komiya, T.: Water content of the mantle xenoliths from Kimberley and implications for explaining textural variations in cratonic roots, Geol. J., 46, 173–182, doi:10.1002/gj.1216, 2011.

Karato, S., Jung, H., Katayama, I., and Skemer, P.: Geodynamics significance of seismic anisotropy of the upper mantle: New insights from laboratory studies, Annu. Rev. Earth Planet Sci., 36, 59–95, https://doi.org/10.1146/annurev.earth.36.031207.124120, 2008.

Kats, A.: Hydrogen in alpha quartz. Philips Res, Rep. 17, 133–195, 201–279, 1962.

Kerrich, R.: Some effects of tectonic recrystallisation on fluid inclusions in vein quartz, Contrib. Mineral. Petrol., 59, 195–202, https://doi.org/10.1007/BF00371308, 1976.

Kilian, R., Heilbronner, R., Holyoke III, C. W., Kronenberg, A. K., and Stünitz, H.: Dislocation creep of dry quartz. J. Geophys. Res. Solid Earth, 121, 3278–3299, https://doi.org/10.1002/2015JB012771, 2016.

https://doi.org/10.5194/egusphere-2022-1487
Preprint. Discussion started: 2 January 2023

Koch, P. S., Christie, J. M., Ord, A., and George, R. P. Jr.: Effect of water on the rheology of experimentally deformed quartzite, J. Geophys. Res. Solid Earth, 94, 13975–13996, https://doi.org/10.1029/JB094iB10p13975, 1989.

Kohlstedt, D. L., Evans, B., and Mackwell, S. J.: Strength of the lithosphere: Constraints imposed by laboratory experiments, J. Geophys. Res., 100(B9), 17587–17602, https://doi.org/10.1029/95JB01460, 1995.

Kronenberg, A. K.: Hydrogen speciation and chemical weakening of quartz, Rev. Mineral. Geochem., 29, 123–176, https://doi.org/10.1515/9781501509698-009, 1994.

Kronenberg, A. K., Ashley, K. T., Francsis, M. K., Holyoke III, C. W., Jezek, L., Kronenberg, J. A., Law, R. D., and Thomas, J. B.: Water loss during dynamic recrystallization of Moine thrust quartzites, northwest Scotland, Geology, 48(6), 557–561, https://doi.org/10.1130/G47041.1, 2020.

Kronenberg, A. K., Hasnan, H. F. B., Holyoke III, C. W., Law, R. D., Liu, Z., and Thomas, J. B.: Synchrotron FTIR imaging of OH in quartz mylonites, Solid Earth, 8, 1025–1045, https://doi.org/10.5194/se-8-1025-2017, 2017.

Kronenberg, A. K., Kirby, S. H., Aines, R. D., and Rossman, G. R.: Solubility and diffusional uptake of hydrogen in quartz at high water pressures: Implications for hydrolytic weakening, J. Geophys. Res. Solid Earth, 91, 12723–12744, https://doi.org/10.1029/JB091iB12p12723, 1986.

Kronenberg, A. K., Segall, P., and Wolf, G. H.: Hydrolytic weakening and penetrative deformation within a natural shear zone, in: The Brittle–Ductile Transition in Rocks, edited by: Duba, A. G., Durham, W. B., Handin, J. W., and Wang, H. F., American Geophysical Union, Washington DC, 21–36, https://doi.org/10.1029/GM056p0021, 1990.

Kronenberg, A. K. and Tullis, J.: Flow strengths of quartz aggregates: Grain size and pressure effects due to hydrolytic weakening, J. Geophys. Res. Solid Earth, 89, 4281–4297, https://doi.org/10.1029/JB089iB06p04281, 1984.

Kronenberg, A. K. and Wolf, G. H.: Fourier transform infrared spectroscopy determinations of intragranular water content in quartz-bearing rocks: Implications for hydrolytic weakening in the laboratory and within the earth, Tectonophysics, 172, 225–271, https://doi.org/10.1016/0040-1951(90)90034-6, 1990.

https://doi.org/10.5194/egusphere-2022-1487
Preprint. Discussion started: 2 January 2023

Libowitzky, E. and Rossman, G. R.: An IR absorption calibration for water in minerals, Am. Mineral, 82, 1111–1115, https://doi.org/10.2138/am-1997-11-1208, 1997.

Lu, L. X. and Jiang, D.: Quartz flow law revisited: The significance of pressure dependence of the activation enthalpy, J. Geophys. Res. Solid Earth, 124, 241–256, https://doi.org/10.1029/2018JB016226, 2019.

Lusk, A. D. J., Platt, J. P., and Platt, J. A.: Natural and experimental constraints on a flow law for dislocation-dominated creep in wet quartz, Geophys. Res. Solid Earth, 126, e2020JB021302, https://doi.org/10.1029/2020JB021302, 2021.

Masuti, S., Karato, S., Girard, J., and Barbot, S. D.: Anisotropic high-temperature creep in hydrous olivine single crystals and its geodynamic implications, Phys. Earth Planet. Inter., 290, 1–9, https://doi.org/10.1016/j.pepi.2019.03.002, 2019.

Menegon, L., Nasipuri, P., Stünitz, H., Behrens, H., and Ravna, E.: Dry and strong quartz during deformation of the lower crust in the presence of melt, J. Geophys. Res. Solid Earth, 116, B10410, https://doi.org/10.1029/2011JB008371, 2011.

Muto, J., Nagahama, H., and Hashimoto, T.: Micro-infrared reflection spectroscopic mapping: application to the detection of hydrogen-related species in natural quartz, J. Microsc., 216, 222–228, https://doi.org/10.1111/j.0022-2720.2004.01419.x, 2004.

Muto, J., Nagahama, H., and Hashimoto, T.: Water distribution in dynamically recrystallized quartz grains: cathodoluminescence and micro-infrared spectroscopic mapping, in: High-strain zones: Structure and physical properties, edited by: Bruhn, D. and Durlini, L., Geol. Soc. London Spec. Publ., 245, 397–407, https://doi.org/10.1144/GSL.SP.2005.245.01.19, 2005.

Nakashima, S., Matayoshi, H., Yuko, T., Michibayashi, K., Masuda, T., Kuroki, N., Yamagishi, H., Ito, Y., Nakamura, A.: Infrared microspectroscopy analysis of water distribution in deformed and metamorphosed rocks, Tectonophysics, 245, 263–276, https://doi.org/10.1016/0040-1951(94)00239-6, 1995.

Niimi, N., Aikawa, N., and Shinoda, K.: The infrared absorption band at 3596 cm^{-1} of the recrystallized quartz from Mt. Takamiyama, southwest Japan, Mineral. Mag., 63, 693–701, https://doi.org/10.1180/002646199548853, 1999.

Oide, K. and Fujita, Y.: Geology of the Iwanuma District. With geological sheet map at 1:50,000, Geol. Surv. Japan, 31 p. (in Japanese with English Abstract), 1975.

https://doi.org/10.5194/egusphere-2022-1487
Preprint. Discussion started: 2 January 2023

O'kane, A., Onasch, C. M., and Farver, J. R.: The role of fluids in low temperature, fault related deformation of quartz arenite, J. Struct. Geol., 29, 819–836, https://doi.org/10.1016/j.jsg.2007.01.003, 2007.

Palazzin, G., Raimbourg, H., Stüunitz, H., Heilbronner, R., Neufeld, K., and Précigout, J.: Evolution in H_2O contents during deformation of polycrystalline quartz: An experimental study, J. Struct. Geol., 114, 95–110, https://doi.org/10.1016/j.jsg.2018.05.021, 2018.

Parrish, D. K., Krivz, A. L., and Carter, N. L.: Finite-element folds of similar geometry, Tectonophysics, 32, 183–207, https://doi.org/10.1016/0040-1951(76)90062-7, 1976.

Passchier, C. W. and Trouw, R. A. J.: Microtectonics, 2nd Ed. Springer-Verlag, Heidelberg, 2005.

Paterson, M. S.: The determination of hydroxyl by infrared absorption in quartz, silicate glasses and similar materials, Bull. Minéral., 105, 20–29, 1982.

Post, A., Tullis, J., and Yund, R. A.: Effects of chemical environment on dislocation creep of quartzite. J. Geophys. Res. Solid Earth, 101, 22143–22155, https://doi.org/10.1029/96JB01926, 1996.

Rutter, E. H. and Brodie, K. H.: The role of tectonic grain size reduction in the rheological stratification of the lithosphere, Geol. Rundsch., 77(1), https://doi.org/10.1007/BF01848691, 295–308, 1988.

Shimizu, I.: Theories and applicability of grain size piezometers: The role of dynamic recrystallization mechanisms, J. Struct. Geol., 30:899–917. https://doi.org/10.1016/j.jsg.2008.03.004, 2008.

Shimizu, I.: Steady-state grain size in dynamic recrystallization of minerals, in: Recrystallization, edited by: Sztwiertnia, K., InTech, Rijeka, Croatia, 371–386, doi:10.5772/33701, 2012.

Skemer, P., Warren, J. M., Hansen, L. N., Hirth, G., and Kelemen, P. B.: The influence of water and LPO on the initiation and evolution of mantle shear zones, Earth Planet. Sci. Lett., 375, 222–233, http://dx.doi.org/10.1016/j.epsl.2013.05.034, 2013.

Stalder, R.: OH point defects in quartz – a review, Eur. J. Mineral., 33, 145–163, https://doi.org/10.5194/ejm-33-145-2021, 2021.

Stenina, N.G.: Water-related defects in quartz, Bull. Geosci., 79, 251–268, 2004.

Stipp, M. and Tullis, J.: The recrystallized grain size piezometer for quartz, Geophys. Res. Lett., 30, 2003. https://doi.org/10.1029/2003GL018444, 2003.

https://doi.org/10.5194/egusphere-2022-1487
Preprint. Discussion started: 2 January 2023

Stipp, M., Stünitz, H., Heilbronner, R., and Schmid, S. M.: The eastern Tonale fault zone: a "natural laboratory" for crystal plastic deformation of quartz over a temperature range from 250 to 700 degrees C, J. Struct. Geol., 24, 1861–1884, https://doi.org/10.1016/S0191-8141(02)00035-4, 2002.

Stipp, M., Tullis, J., and Behrens, H.: Effect of water on the dislocation creep microstructure and flow stress of quartz and implications for the recrystallized grain size piezometer, J. Geophys. Res. Solid Earth, 111, B04201, https://doi.org/10.1029/2005JB003852, 2006.

Stünitz, H., Thust, A., Heilbronner, R., Behrens, H., Kilian, R., Tarantola, A., and Fitz Gerald, J. D.: Water redistribution in experimentally deformed natural milky quartz single crystals–Implications for H_2O-weakening processes. J. Geophys. Res. Solid Earth, 122, 866–894, https://doi.org/10.1002/2016JB013533, 2017.

Thomas, S. M., Koch–Müller, M., Reichart, P., Rhede, D., Thomas, R., Wirth, R., and Matsyuk, S.: IR calibrations for water determination in olivine, r-GeO_2, and SiO_2 polymorphs, Phys. Chem. Miner., 36, 489–509, https://doi.org/10.1007/s00269-009-0295-1, 2009.

Tokle, L., Hirth, G., and Behr, W.M.: Flow laws and fabric transitions in wet quartzite, Earth Planet. Sci. Lett., 505, 152–161, https://doi.org/10.1016/j.epsl.2018.10.017, 2019.

Tarantola, A., Diamond, L. W., and Stünitz, H.: Modification of fluid inclusions in quartz by deviatoric stress I: experimentally induced changes in inclusion shapes and microstructures, Contrib. Mineral. Petrol., 160, 825–843. https://doi.org/10.1007/s00410-010-0509-z, 2010.

Tsuchiya, N., Ohtomo,Y., Takeda, T., Sasaki, J., and Abe, M.: Late Carboniferous and Early Cretaceous adakitic granites from eastern margin of the Abukuma Mountains, Jour. Geol. Soc. Japan, 119, Supplement, 154–167, (in Japanese with English Abstract), doi:10.5575/geosoc.2013.0033, 2013.

Tsuchiya, N., Takeda, T., Tani, K., Adachi, T., Nakano, N., Osanai, Y., and Kimura, J.: Zircon U–Pb age and its geological significance of late Carboniferous and Early Cretaceous adakitic granites from eastern margin of the Aubukuma Mountains, Japan, Jour. Geol. Soc. Japan, 120, No. 2, 37–51, doi:10.5575/geosoc.2014.0003, 2014.

Trepied, L. and Doukhan, J. C.: Dissociated 'a' dislocations in quartz, J. Mater. Sci., 13, https://doi.org/10.1007/BF00541797, 492–498, 1978.

Tullis, J.: Deformation of granitic rocks: Experimental studies and natural examples, Rev. Mineral. Geochem., 51, 51–95, https://doi.org/10.2138/gsrmg.51.1.51, 2002.

https://doi.org/10.5194/egusphere-2022-1487
Preprint. Discussion started: 2 January 2023

Twiss, R. J.: Theory and applicability of recrystallized grain size paleopiezometer, Pure Appl. Geophys., 115, 227–244, https://doi.org/10.1007/978-3-0348-5745-1_13, 1977.

Vityk, M. O., Bodnar, R. J., and Doukhan, J. C.: Synthetic fluid inclusions. XV. TEM investigation of plastic flow associated with reequilibration of fluid inclusions in natural quartz, Contrib. Mineral. Petrol., 139, 285–297, https://doi.org/10.1007/s004100000142, 2000.

Watson, E. B. and Brenan, J. M: Fluids in the lithosphere, 1. Experimentally-determined wetting characteristics of CO_2-H_2O fluids and their implications for fluid transport, host-rock physical properties, and fluid inclusion formation, Earth Planet. Sci. Lett., 85, 497–515, https://doi.org/10.1016/0012-821X(87)90144-0, 1987.

Wilkins, R. W. T. and Barkas, J. P.: Fluid inclusions, deformation and recrystallization in granite tectonites, Contrib. Mineral. Petrol., 65, 293–299, https://doi.org/10.1007/BF00375515, 1978.

https://doi.org/10.5194/egusphere-2022-1487
Preprint. Discussion started: 2 January 2023

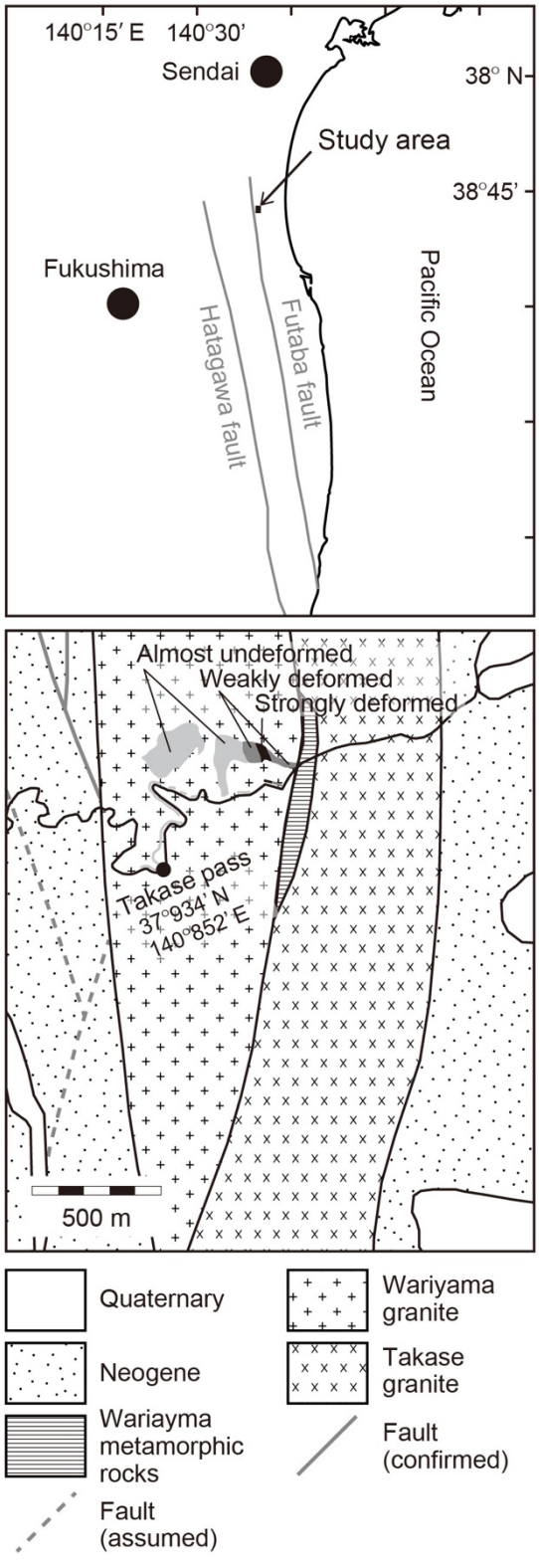

https://doi.org/10.5194/egusphere-2022-1487
Preprint. Discussion started: 2 January 2023

Figure 1. Study area location map and geological map after Oide and Fujita (1975), Fujita et al. (1988), and Tsuchiya et al. (2014). The Wariyama granite was categorized into three types based on the degree of deformation, as determined by the naked eye (Fig. 2) and by microstructures observed under a polarizing microscope (Fig. 3). The three types are referred to as "almost undeformed", "weakly deformed", and "strongly deformed", with distributions as shown in the geological map.

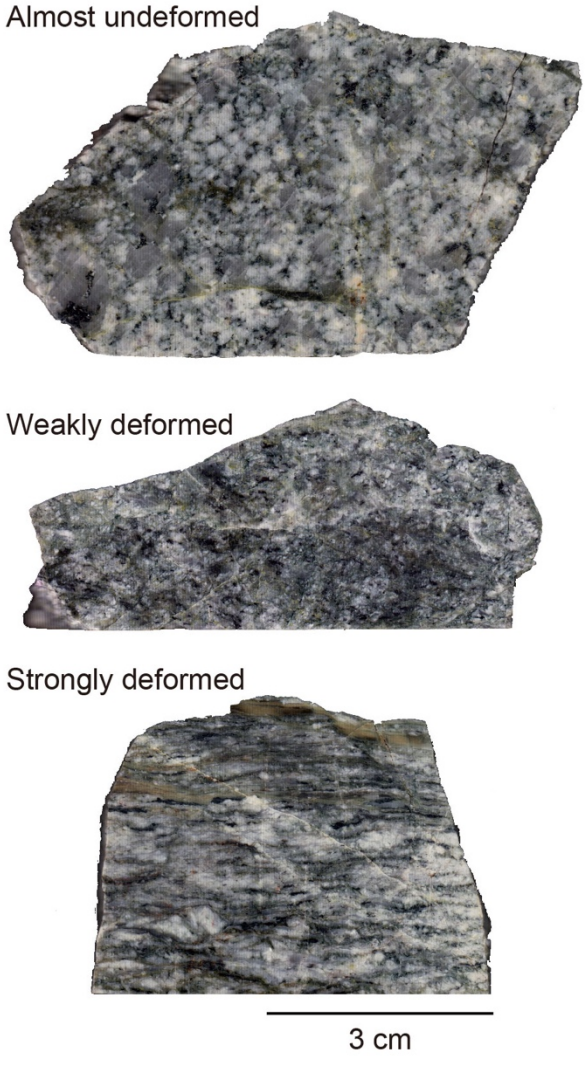

Figure 2. Scanned images of the three studied samples of the Wariyama granite. The two deformed samples were cut parallel to the lineation and perpendicular to the foliation.

https://doi.org/10.5194/egusphere-2022-1487
Preprint. Discussion started: 2 January 2023

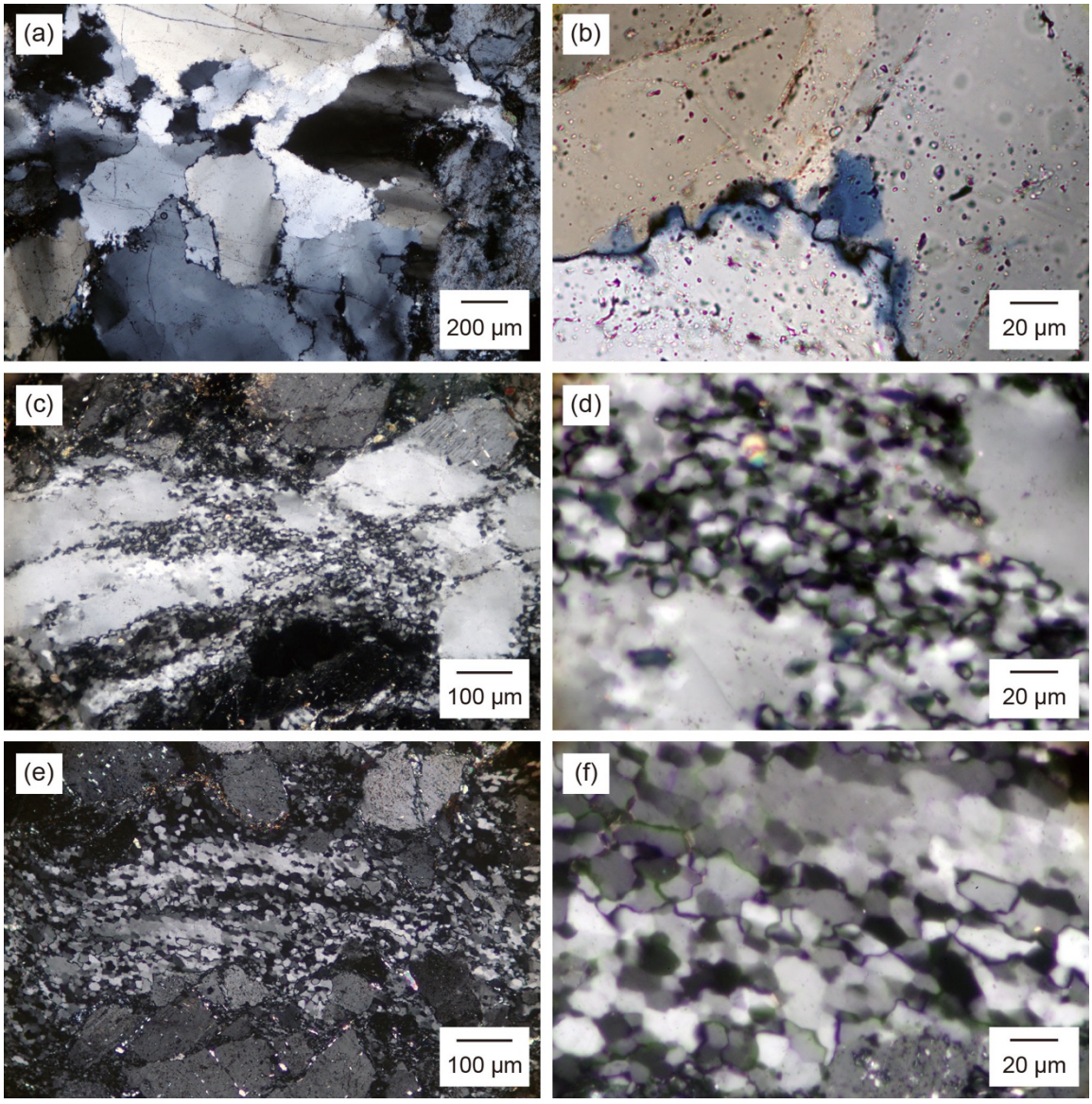

Figure 3. Optical photomicrographs taken under cross-polarized light showing quartz textures in the Wariyama granite. (a and b) Almost undeformed sample. Quartz grain boundaries are wavy, and a few bulged grains are observed. (c and d) Weakly deformed sample cut parallel to the lineation and perpendicular to the foliation. Regions of bulged quartz grains are a few hundred micrometers in size, and adjacent host grains are elongated. (e and f) Strongly deformed sample cut parallel to the lineation and perpendicular to the foliation. Almost all quartz grains are recrystallized by subgrain rotation, and subgrains remain in some regions, as in the upper part of (f).

https://doi.org/10.5194/egusphere-2022-1487
Preprint. Discussion started: 2 January 2023

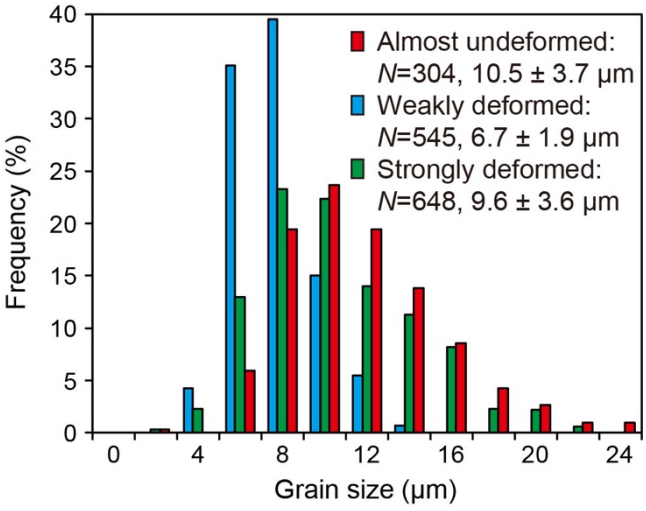

590 **Figure 4. Grain size distributions of recrystallized quartz grains of the studied samples with three different degrees of deformation. *N* is the number of grains measured. Mean grain sizes and standard deviations are given.**

https://doi.org/10.5194/egusphere-2022-1487
Preprint. Discussion started: 2 January 2023

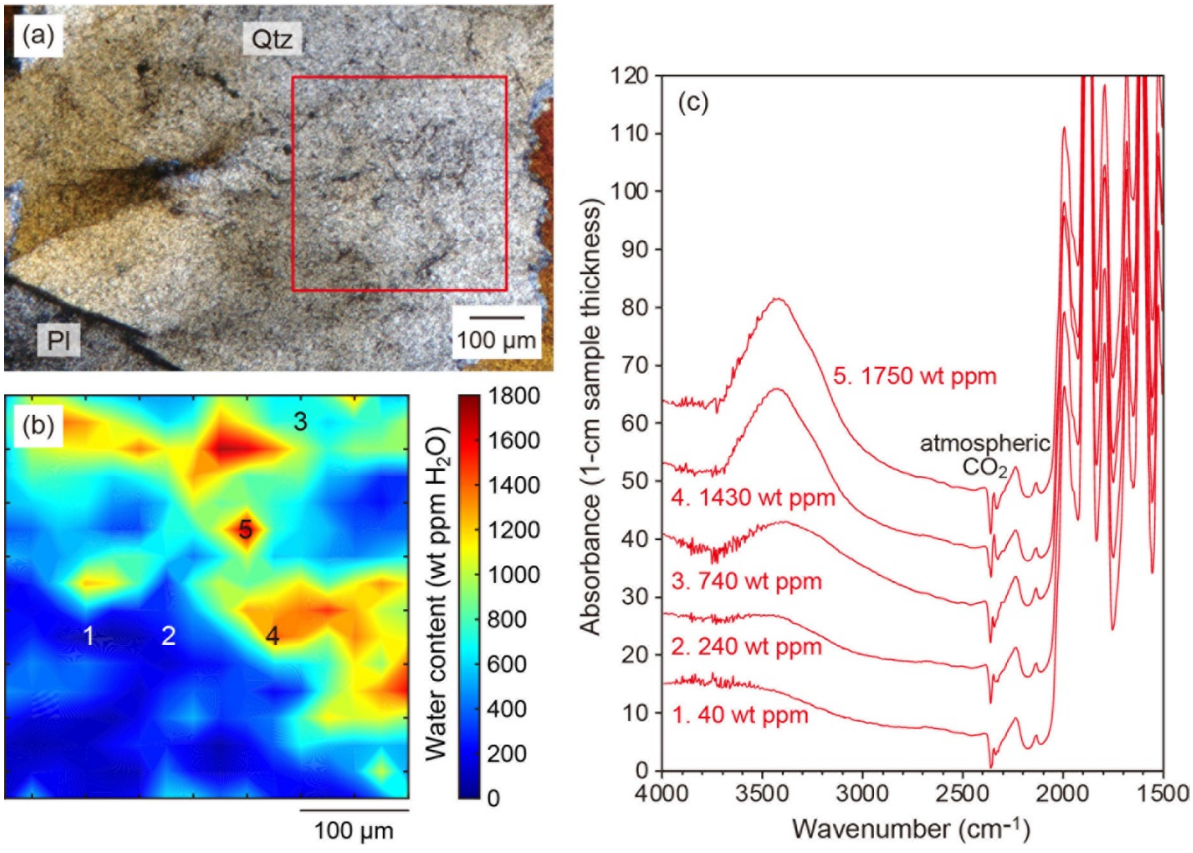

595 **Figure 5. IR mapping results for the almost undeformed sample. The sample thickness is 60 μm. (a) Optical photomicrograph under cross-polarized light. The IR mapped area is shown with a red square. (b) Water distribution. Numbers represent raw IR spectra in (c) from low to high water contents.**

https://doi.org/10.5194/egusphere-2022-1487
Preprint. Discussion started: 2 January 2023

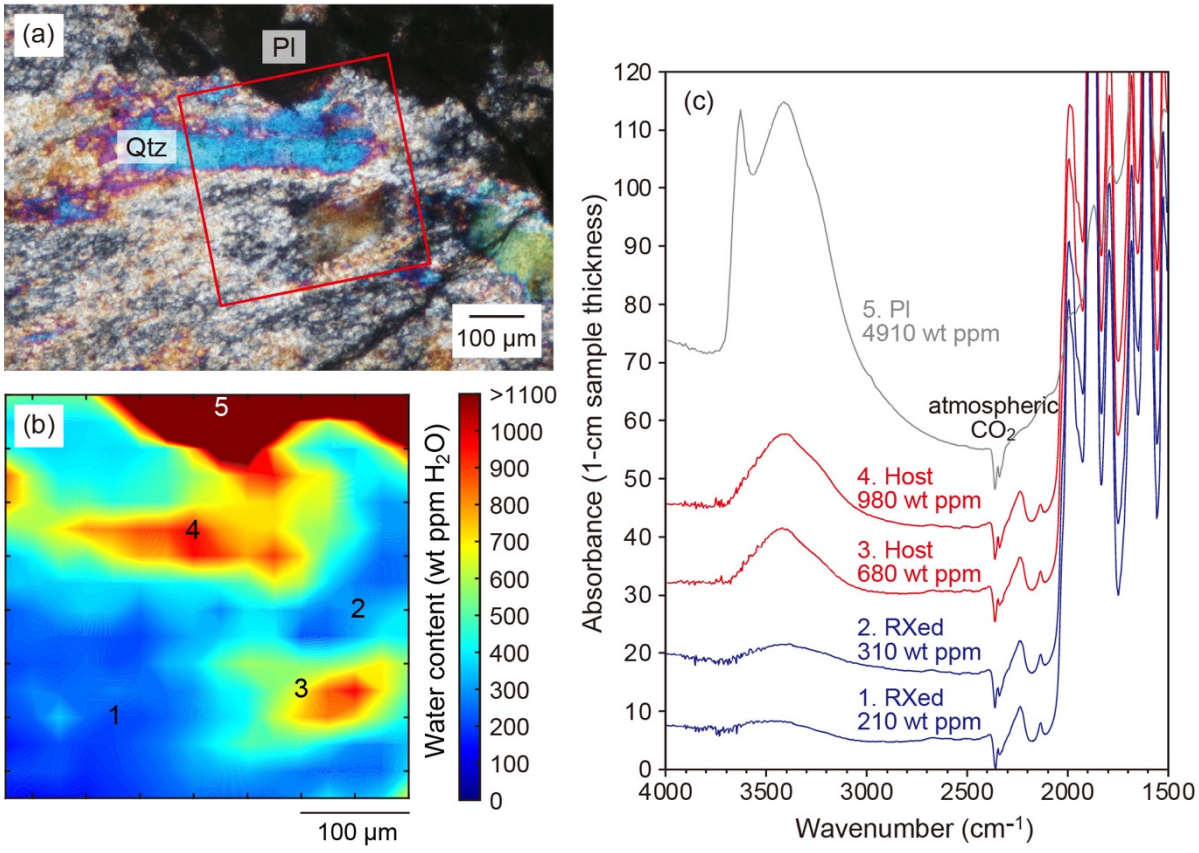

Figure 6. IR mapping results for the weakly deformed sample. The sample thickness is 103 μm. (a) Optical photomicrograph under cross-polarized light. The IR mapped area is shown with a red square. (b) Water distribution. Numbers represent raw IR spectra in (c). Color-coded water contents up to 1100 wt. ppm H_2O are for quartz, and those above are for plagioclase around No. 5 in (b). "RXed" in (c) means "recrystallized".

https://doi.org/10.5194/egusphere-2022-1487
Preprint. Discussion started: 2 January 2023

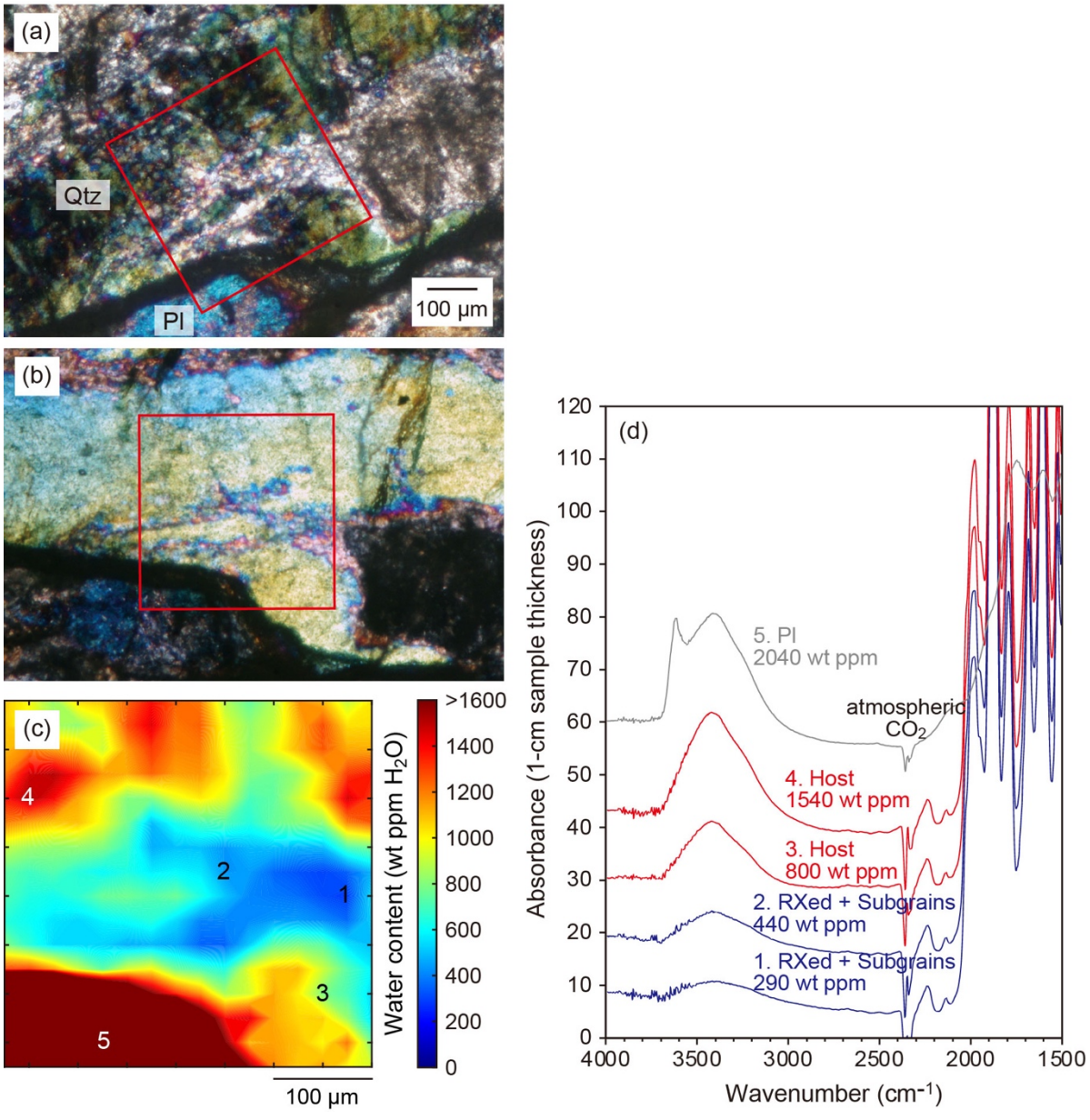

Figure 7. IR mapping results for the weakly deformed sample. The sample thickness is 97 μm. (a) Optical photomicrograph under cross-polarized light. The IR mapped area is shown with a red square. (b) Optical photomicrograph rotated approximately 30° clockwise from (a). Fine-graind quartz regions are smaller than those in (a), indicating subgrains are included. (c) Water distribution. Numbers represent raw IR spectra in (c). Color-coded water contents up to 1600 wt. ppm H_2O are for quartz, and those above are for plagioclase around No. 5 in (b). "RXed" in (d) means "recrystallized". Both recrystallized grains and subgrains are included in the measured area.

https://doi.org/10.5194/egusphere-2022-1487
Preprint. Discussion started: 2 January 2023

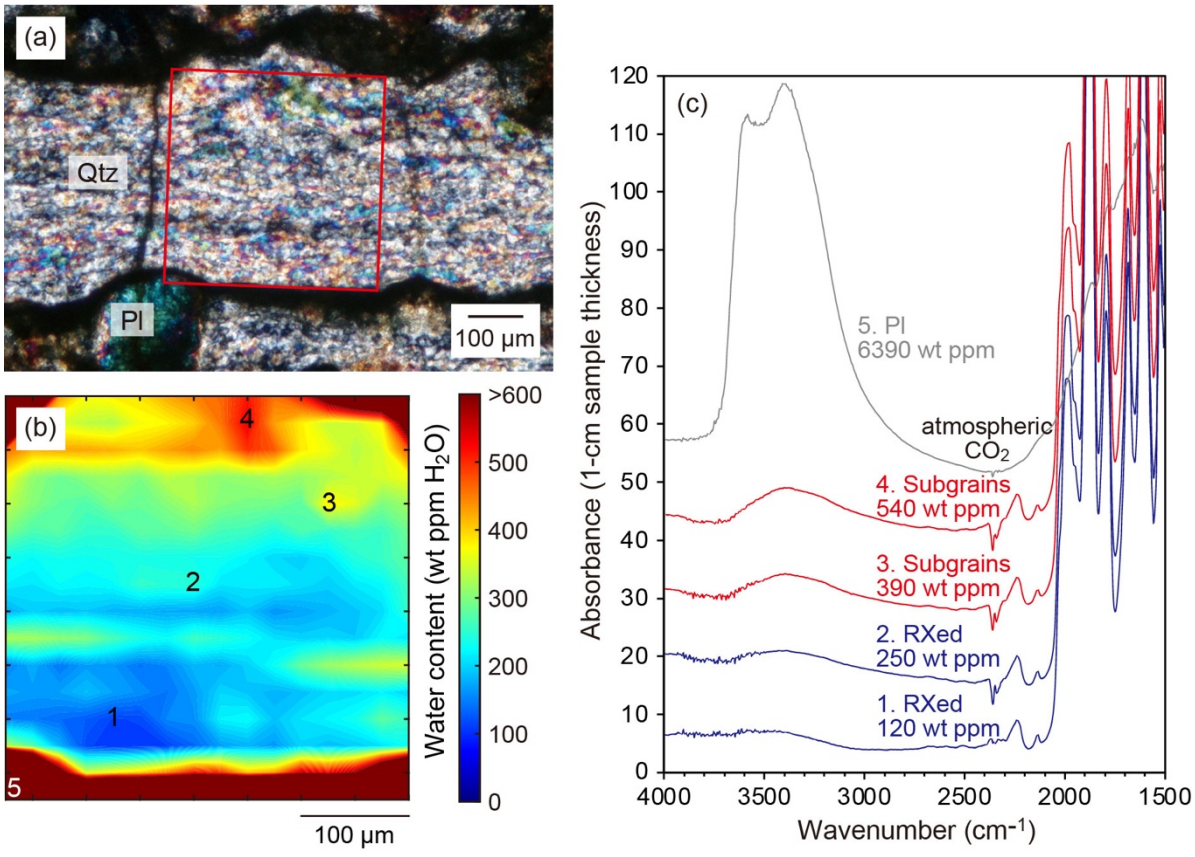

Figure 8. IR mapping results for the strongly deformed sample. The sample thickness is 112 µm. (a) Optical photomicrograph under cross-polarized light. The IR mapped area is shown with a red square. (b) Water distribution. Numbers represent raw IR spectra in (c). Color-coded water contents up to 600 wt. ppm H_2O are for quartz, and those above are for plagioclase and phyllosilicate around No. 5 and others in (b). Quartz subgrains in host grains are around Nos 3 and 4 in (b), which correspond to the microstructure in (a). "RXed" in (c) means "recrystallized".

https://doi.org/10.5194/egusphere-2022-1487
Preprint. Discussion started: 2 January 2023

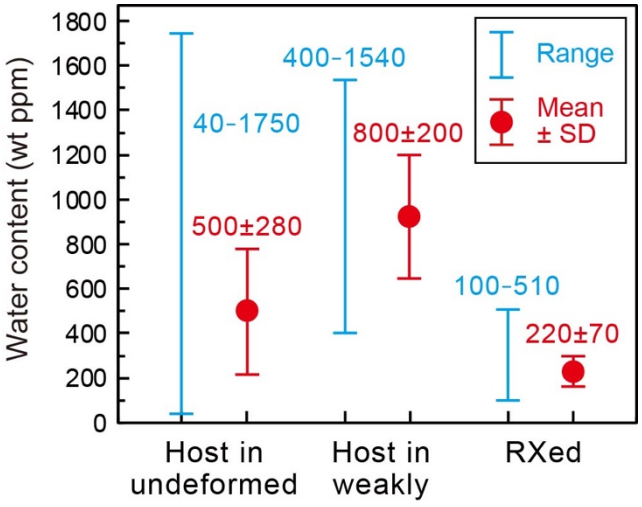

Figure 9. Summary of water content variations in quartz. "Host" represents host quartz grains as intracrystalline parts in the almost undeformed and weakly deformed samples. These two samples are referred to as "undeformed" and "weakly" in the figure, respectively. "RXed" represents regions of recrystallized quartz grains including both intracrystalline parts and grain boundaries in the weakly deformed and strongly deformed samples. Ranges from the lowest to highest contents in blue and means with standard deviations (SD) in red are shown. The difference in water contents in host grains between the almost undeformed and weakly deformed samples may be because of the areas to be measured. In addiction, the water distributions in host grains in the latter sample are comparable with the shapes of host grains but those in the former sample are not (Figs 5–7). Therefore, there may be a redistribution of water in host grains by plastic deformation, as supported by the photomicrographs which show less visible fluid inclusions in the latter sample (Fig. 3).